

# *The influence of weather regimes on European renewable energy production and demand*

Article

Accepted Version

Creative Commons: Attribution 3.0 (CC-BY)

van der Wiel, K., Bloomfield, H., Lee, R. W., Stoop, L., Blackport, R., Screen, J. and Selten, F. M. (2019) The influence of weather regimes on European renewable energy production and demand. *Environmental Research Letters*. ISSN 1748-9326 doi: <https://doi.org/10.1088/1748-9326/ab38d3> (In Press) Available at <http://centaur.reading.ac.uk/85447/>

It is advisable to refer to the publisher's version if you intend to cite from the work. See [Guidance on citing](#).

To link to this article DOI: <http://dx.doi.org/10.1088/1748-9326/ab38d3>

Publisher: IOP Publishing Ltd

All outputs in CentAUR are protected by Intellectual Property Rights law, including copyright law. Copyright and IPR is retained by the creators or other copyright holders. Terms and conditions for use of this material are defined in the [End User Agreement](#).

[www.reading.ac.uk/centaur](http://www.reading.ac.uk/centaur)

## **CentAUR**

Central Archive at the University of Reading

Reading's research outputs online

# The influence of weather regimes on European renewable energy production and demand

Karin van der Wiel<sup>1</sup>, Hannah C. Bloomfield<sup>2</sup>, Robert W. Lee<sup>2,3</sup>,  
Laurens P. Stoop<sup>4,5</sup>, Russell Blackport<sup>6</sup>, James A. Screen<sup>6</sup>,  
Frank M. Selten<sup>1</sup>

<sup>1</sup> Royal Netherlands Meteorological Institute, De Bilt, the Netherlands

<sup>2</sup> University of Reading, Department of Meteorology, Reading, United Kingdom

<sup>3</sup> National Centre for Atmospheric Science, Reading, United Kingdom

<sup>4</sup> Utrecht University, Research Institute of Informatics and Computer Science,  
Utrecht, the Netherlands

<sup>5</sup> Utrecht University, Copernicus Institute of Sustainable Development, Utrecht, the  
Netherlands

<sup>6</sup> University of Exeter, College of Engineering, Mathematics and Physical Sciences,  
Exeter, United Kingdom

E-mail: [wiel@knmi.nl](mailto:wiel@knmi.nl)

July 2019

**Abstract.** The growing share of variable renewable energy increases the meteorological sensitivity of power systems. This study investigates if large-scale weather regimes capture the influence of meteorological variability on the European energy sector. For each weather regime, the associated changes to wintertime -mean and extreme- wind and solar power production, temperature-driven energy demand and energy shortfall (residual load) are explored. Days with a blocked circulation pattern, i.e. the Scandinavian Blocking and NAO negative regimes, on average have lower than normal renewable power production, higher than normal energy demand and therefore, higher than normal energy shortfall. These average effects hide large variability of energy parameters within each weather regime. Though the risk of extreme high energy shortfall events increases in the two blocked regimes (by a factor of 2.0 and 1.5, respectively), it is shown that such events occur in all regimes. Extreme high energy shortfall events are the result of rare circulation types and smaller-scale features, rather than extreme magnitudes of common large-scale circulation types. In fact, these events resemble each other more strongly than their respective weather regime mean pattern. For (sub-)seasonal forecasting applications weather regimes may be of use for the energy sector. At shorter lead times or for more detailed system analyses, their ineffectiveness at characterising extreme events limits their potential. (213 words)

*Keywords:* Energy meteorology, Energy transition, Renewable energy, Weather regimes, Wind energy, Solar energy, Energy demand

Submitted to: *Environ. Res. Lett.*

## 1. Introduction

To mitigate future climate change an energy transition to low or zero-carbon energy sources is required (e.g. Matthews et al., 2009; Meinshausen et al., 2009). For this reason, in many places the share of renewable wind and solar power generation of total power generation is increasing. This growing share of variable renewable energy increases the sensitivity of power systems to meteorological conditions and their variability. Wind and solar electricity production, and also electricity demand all depend on the weather and therefore exhibit variability at hourly, daily, weekly, seasonal and annual timescales (e.g. Kavak Akpınar and Akpınar, 2005; Pryor et al., 2006; Sinden, 2007; Suri et al., 2007; Bessec and Fouquau, 2008; Bloomfield et al., 2016). It is paramount to consider the spatial and temporal variations in energy production and energy demand in the design and operation of future power systems with a high share of renewable sources (Armaroli and Balzani, 2011; Zeyringer et al., 2018).

To guarantee a continuous and secure energy supply in a future highly-renewable power system, critical situations require special attention. In Europe, large-scale high pressure systems can lead to the unfortunate combination of low wind and solar power production and high energy demand, resulting in extreme high energy shortfall (Bloomfield et al., 2018; Van der Wiel et al., 2019a). The flexibility requirements of a power system are, in part, determined by such events (Huber et al., 2014). System adequacy analyses, e.g. the ability to meet peak demand, taking into account the full range of meteorological variability and power system characteristics are thus essential to identify, and design for, critical events (Armaroli and Balzani, 2011).

To meet the societal need for information on the dependence of energy production and energy demand on weather and climate, an interdisciplinary scientific discipline is developing rapidly: “energy meteorology”. The meteorological community has contributed with insights into the effects of interannual meteorological variability on energy production and demand (Klink, 2002; Pryor et al., 2006; Davy and Troccoli, 2012; Haupt et al., 2016; Kumler et al., 2018), the influence of the North Atlantic Oscillation (NAO, e.g. Pozo-Vázquez et al., 2004; Brayshaw et al., 2011; Ely et al., 2013; Jerez et al., 2013; Curtis et al., 2016; Zubiate et al., 2017; Ravestein et al., 2018), expected changes due to further climate change (Pryor and Barthelmie, 2010; Hueging et al., 2013; Jerez et al., 2015b; Haupt et al., 2016; Reyers et al., 2016; Craig et al., 2019), and the seasonal predictability of energy-related variables (Clark et al., 2017; Thornton et al., 2019). However, the relationship between meteorology, energy impacts, and critical events is complex and therefore needs tailored studies.

This study aims to investigate whether weather regimes adequately represent the influence of meteorological variations on the European energy sector. Weather regimes are classifications of common atmospheric circulation regimes (Figure 1) and have proven to be useful in weather forecasting and climate change applications (e.g Reinhold, 1987; Ferranti et al., 2015; Neal et al., 2016; Matsueda and Palmer, 2018). They influence the weather at the surface (e.g. Trigo and DaCamara, 2000; Plaut and Simonnet, 2001; Yiou and Nogaj, 2004; Santos et al., 2005; Yiou et al., 2008; Donat et al., 2010), hence influencing renewable power generation and electricity demand (Grams et al., 2017; Thornton et al., 2017). Meteorological and energy forecasts are of value for the energy sector, that plans operations and resource adequacy, and trade on electricity markets based in part on this information (Pinson et al., 2013). Specifically, this study answers two questions: i) What are the average impacts of the weather regimes on energy variables? and ii) Are energy extremes linked to a specific weather regime? We quantify the day-to-day variability of energy variables and the risk of extreme or critical events in each weather regime. Our focus is on the winter season, in which the weather regimes (Sanchez-

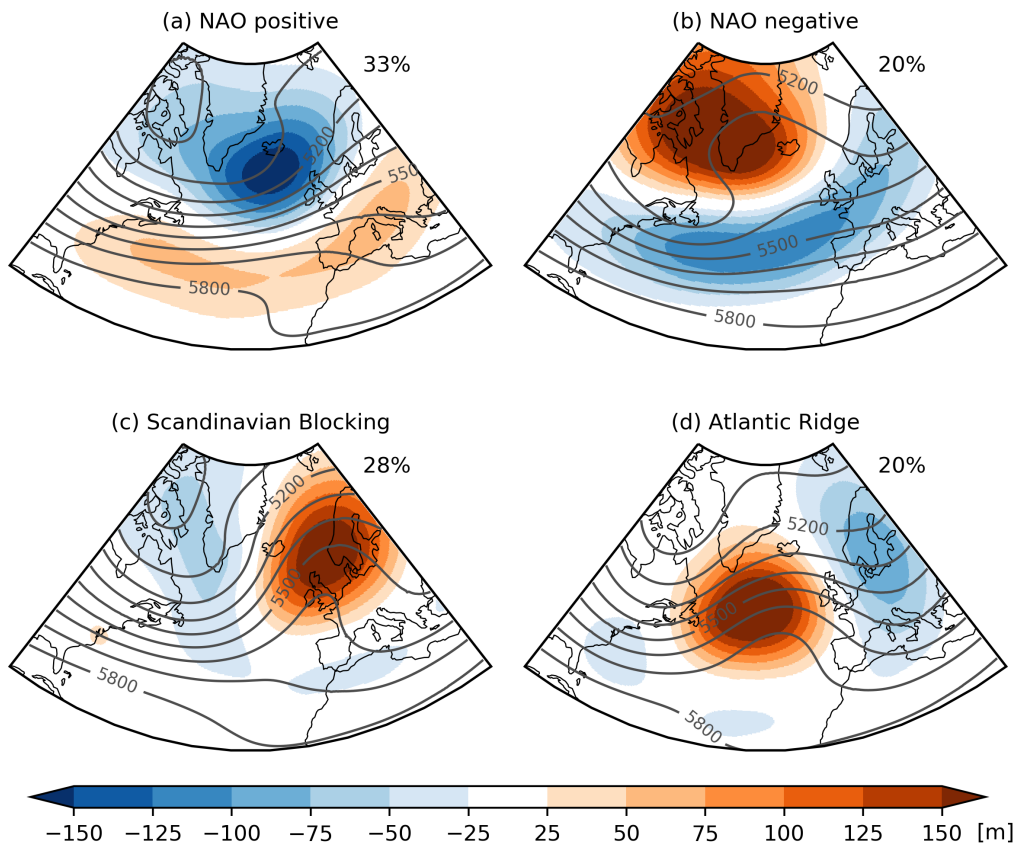


**Figure 1.** Four regimes of atmospheric circulation in the North Atlantic-European domain, (a) NAO positive, (b) NAO negative, (c) Scandinavian Blocking, (d) Atlantic Ridge. Colours show the 500 hPa height anomaly [m], contour lines show the 500 hPa height [m, interval 100 m] indicative of the direction of flow. The percentage values denote the percentage of total days categorised in each regime. Figure based on ERA5 data (DJF, 1979-2018).

85 Gomez et al., 2009; Lavaysse et al., 2018) and the variability of total wind and solar energy  
 86 production and demand (Van der Wiel et al., 2019a, their Figure 8) are most pronounced. We  
 87 take a compound system approach, taking into account the combined effects of wind and solar  
 88 power production, and energy demand.

## 89 2. Methods

### 90 2.1. Meteorological data

91 We used the ERA5 reanalysis product (Copernicus Climate Change Service, 2017) to represent  
 92 observed historical meteorological conditions (Olauson, 2018; Urraca et al., 2018; Ramon et al.,  
 93 2019). The full ERA5 record available at time of analysis was used, 1979-2018, providing  
 94 40 years of data. The analysis of variability, in particular for the occurrence of extreme events,  
 95 is hindered by the limited length of the observed record (Bloomfield et al., 2016; Van der  
 96 Wiel et al., 2019a). In the 40 year ERA5 record just four 1-in-10 year extreme events can  
 97 be sampled. We therefore also used data from two large ensemble experiments created using  
 98 two Global Climate Models (GCMs): EC-Earth (v2.3, Hazeleger et al., 2012) and HadGEM2-

99 ES (Martin et al., 2011). Each large ensemble experiment contains 2000 years of simulated  
100 weather for present-day conditions. This allows an analysis of how 200 extreme events in each  
101 model dataset, with return periods of 10 years and longer, are distributed over the different  
102 weather regimes. Details on the large ensemble GCM experimental setup are provided in  
103 Van der Wiel et al. (2019b) and Blackport and Screen (2019). The GCMs reproduce the  
104 observed temporal occurrence, surface impacts and variability of/within weather regimes (see  
105 Supporting Information, SI).

## 106 *2.2. Weather regime classification*

107 Each winter day (December, January, February, DJF) in the ERA5 record was assigned to  
108 one of the four North Atlantic weather regimes (Michelangeli et al., 1995; Vautard, 1990)  
109 following the classification method of Cassou (2008). Clustering was done based on daily maps  
110 of anomalous 500 hPa geopotential height [units: m] in the North Atlantic-European region  
111 (90°W-30°E, 20°-80°N). The first fourteen Empirical Orthogonal Functions (EOFs) patterns  
112 were computed (Dawson, 2016), which captured 89 % of total variance. The associated  
113 Principle Component time series (PCs) were used as coordinates of a reduced phase space.  
114 K-means clustering was then used to compute four centroids, and to assign each daily map  
115 to a centroid. The K-means algorithm aims to separate the maps in groups of equal variance  
116 and minimizes the within-cluster sum of squares (Pedregosa et al., 2011).

117 The clustering of GCM data was done in a slightly modified manner. Instead of computing  
118 the EOF patterns from the simulated daily maps itself, the EOF patterns from ERA5 were used  
119 and fourteen pseudo-PCs were computed for each GCM. These pseudo-PCs were then used to  
120 assign each daily map to the centroids as determined from ERA5 data. As expected the spatial  
121 pattern of the resulting weather regimes is similar, the temporal occurrence of each regime  
122 was not constrained and shows agreement between ERA5 and the GCMs (SI Figure S1). The  
123 modified method was applied to ensure maximum spatial similarity of the weather regimes  
124 between the ERA5 data and the GCM data. Physically this is relevant because slight  
125 differences in the location of high/low pressure systems in a regime can have larger impacts  
126 on the surface impacts, and can therefore influence the weather regime-to-energy relation of  
127 interest here.

## 128 *2.3. Energy model*

129 To link the weather regimes to impacts relevant for the energy sector, daily wind and solar  
130 power production and electricity demand were calculated. The energy model used to make  
131 these calculations is described here in brief; for the full model description including model  
132 equations we refer the reader to Van der Wiel et al. (2019a).

133 Spatial patterns of daily wind and solar power potentials [units: %] were considered, a  
134 quantity that depends only on the meteorological state, not on installed wind turbine or solar  
135 cell capacity. Wind power potential was calculated using a power curve profile dependent on  
136 wind speeds (Jerez et al., 2015a), a hub-height of respectively 80 m and 120 m for onshore  
137 and offshore locations is assumed. Solar power potential was calculated using incoming  
138 solar radiation and a solar cell temperature-based performance metric which depended on  
139 temperature, incoming solar radiation and wind speed (TamizhMani et al., 2003), solar panel  
140 tilt is neglected. For the calculation of total European power production [units: TWh day<sup>-1</sup>],  
141 a projected spatial distribution of installed capacity over fifteen western European countries‡

‡ Austria, Belgium, Denmark, France, Germany, Ireland, Italy, Luxembourg, the Netherlands, Norway,

1  
2  
3  
4  
5 142 was assumed (Van der Wiel et al., 2019a).

6 143 Energy demand [in TWh day<sup>-1</sup>] was computed using an regression model calibrated using  
7 144 historical demand data and a population-weighted European mean temperature value (Van der  
8 145 Wiel et al., 2019a). The daily difference between energy demand and renewable wind and solar  
9 146 energy production is referred to as energy shortfall or residual load.

#### 11 12 147 *2.4. Analysis*

13  
14 148 For each of the weather regimes, the average meteorological surface and energy impacts were  
15 149 determined by means of composite analysis, i.e. the mean over all days classified in the regime.  
16 150 Anomalies -departures from normal conditions- were computed by subtracting a DJF-mean  
17 151 climatology. The length of the ERA5 record allowed us to robustly compute the composite  
18 152 mean patterns, the analysis and figures in the main manuscript are therefore based on ERA5  
19 153 data. Equivalent figures for the GCM experiments served as a validation of the simulated data  
20 154 (SI Figures S2, S3).

21  
22 155 We further considered the variability of energy variables within each weather regime. To  
23 156 do so, a systematic comparison of the four regimes to each other and to the full sample, all  
24 157 winter days, was made. Since sampling issues are of concern here, we show both the ERA5  
25 158 data and the GCM data in the main manuscript. We considered extreme events of at least  
26 159 a 10 year return period, it was assumed there are four such events in the 40 year ERA5  
27 160 record and 200 events in each 2000 year GCM experiment. Estimates of change in the risk of  
28 161 occurrence of an extreme event were based on the risk ratio (or probability ratio), a metric  
29 162 commonly used in climate attribution studies:

$$31 \quad 32 \quad 33 \quad 163 \quad RR = \frac{P_{WR}}{P_{clim}} \quad (1)$$

34 164 with  $P_{WR}$  the probability of an extreme event given a weather regime, and  $P_{clim}$  the probability  
35 165 of an extreme event in the full sample.  $RR = 1$  indicates no change in risk,  $RR > 1$  indicates  
36 166 increased risk of an extreme event occurring given that weather regime,  $RR < 1$  indicates  
37 167 decreased risk given that weather regime. Risk ratios noted in the text are averages of the two  
38 168 GCMs.

### 40 41 169 **3. Results**

#### 42 43 170 *3.1. Weather regimes and average meteorological and energy impacts*

44  
45 171 Atmospheric circulation patterns for the four North Atlantic weather regimes are shown  
46 172 in Figure 1. Two regimes resemble the positive and negative phase of the NAO (Hurrell  
47 173 et al., 2003): the ‘NAO positive’ regime (Figure 1a, 33 % of days), characterised by an  
48 174 anomalous low pressure system over Iceland and higher than normal pressure in a band to  
49 175 the south, and the ‘NAO negative’ regime (Figure 1b, 20 % of days), with anomalous high  
50 176 pressure over Greenland/Iceland and lower than normal pressure to the south. A third regime,  
51 177 ‘Scandinavian Blocking’ (Figure 1c, 27 % of days), is characterised by anomalous high pressure  
52 178 over Scandinavia and lower than normal pressure to the south and west. Finally, the fourth  
53 179 regime is distinguished by a positive pressure anomaly over the North Atlantic and a negative  
54 180 anomaly over Europe (Figure 1d, 20 % of days), this regime is referred to as ‘Atlantic Ridge’.  
55 181 These patterns match similar classifications in earlier research (e.g. Vautard, 1990; Michelangeli  
56 182 et al., 1995; Cassou, 2008).

57  
58  
59 Portugal, Spain, Sweden, Switzerland and the United Kingdom  
60

1  
2  
3  
4  
5 183 The anomalous position of pressure systems enhance or disturb the typical zonal, west-to-  
6 184 east, flow. Contour lines in Figure 1 show the flow direction at 500 hPa height. Days classified  
7 185 as NAO positive typically have a stronger than normal zonal flow, in the other regimes the  
8 186 normal zonal flow is weakened over parts of the European continent.

9 187 For energy applications the impacts of the weather regimes at the surface are relevant.  
10 188 The flow at 500 hPa discussed above influences the progression of weather systems over the  
11 189 continent, and therewith influences surface variables such as the near-surface wind speed and  
12 190 temperature. Figure 2 shows the typical surface imprint of the four weather regimes on relevant  
13 191 meteorological variables, while Figure 3 shows the effect on wind and solar power potentials.  
14 192 These anomalies of power potential only lead to changes in power production if wind turbines  
15 193 or solar cells are installed in the region of surface impacts. Subsections 3.1.1 to 3.1.4 describe  
16 194 the mean spatial meteorological and energy characteristics of each regime.

19 195 *3.1.1. NAO positive* The enhanced zonal flow during NAO positive days leads to higher  
20 196 than normal 10 m winds over the North Sea, Denmark, Ireland, the Netherlands and the  
21 197 United Kingdom (Figure 2a). Westerly winds from relatively warm ocean surfaces lead to  
22 198 higher than normal 2 m temperatures in central and northern Europe (Figure 2i). Incoming  
23 199 solar radiation is close to normal for the time of year (Figure 2e).

24 200 These conditions lead to higher than normal wind power potential in the North Sea area  
25 201 (Figure 3a). Over the southern North Sea, the United Kingdom and Denmark the wind power  
26 202 potential is increased by 15 %. Wind power potentials in the Mediterranean Sea are slightly  
27 203 lower than normal. There are no significant changes in solar power potential (Figure 3e).

31 204 *3.1.2. NAO negative* NAO negative days are characterised by an omega block over  
32 205 Greenland and Iceland, leading to reduced zonal flow over the northern half of the European  
33 206 domain (Figure 1b). As a result 10 m wind speeds are lower than normal in the northern North  
34 207 Sea and North Atlantic (Figure 2b), and slightly higher than normal in southern Europe.  
35 208 Incoming radiation is lower than normal in southern Europe (Figure 2f). It is much colder  
36 209 than normal in northern Europe (Figure 2j). The wind power potential is higher than normal  
37 210 over the Mediterranean Sea, Spain and west of Spain, and lower than normal by 5-20 % over  
38 211 the North Sea and North Atlantic (Figure 3b). Solar power potential is lower than normal in  
39 212 the Mediterranean (Figure 3f).

43 213 *3.1.3. Scandinavian Blocking* The anomalous high pressure system over Scandinavia  
44 214 (Figure 1c) reduces the normal zonal flow during Scandinavian Blocking events. 10 m wind  
45 215 speeds over the North Sea, the Celtic Sea and the Bay of Biscay are lower than normal  
46 216 (Figure 2c), incoming solar radiation is higher than normal (Figure 2g). Temperatures over  
47 217 the European main land are lower than normal, it is warmer than normal in the north of  
48 218 Scandinavia (Figure 2k). The spatial pattern of 10 m wind speed anomalies in the Scandinavian  
49 219 Blocking regime somewhat resemble an opposite of the anomalies in the NAO positive regime  
50 220 ( $r = -0.68$ ).

51 221 The reduced wind speeds limit wind power potential over a large region from the western  
52 222 Atlantic up to the Baltic Sea (Figure 3c). Over the North Sea, the United Kingdom and the  
53 223 English Channel wind power potentials are lower by more than 20 %. Solar power potential  
54 224 is higher than normal, most notably over France (Figure 3g).

57 225 *3.1.4. Atlantic Ridge* The fourth regime has the weakest surface impacts for the variables  
58 226 of interest to the energy sector. 10 m wind speeds and 2 m temperatures are close to normal



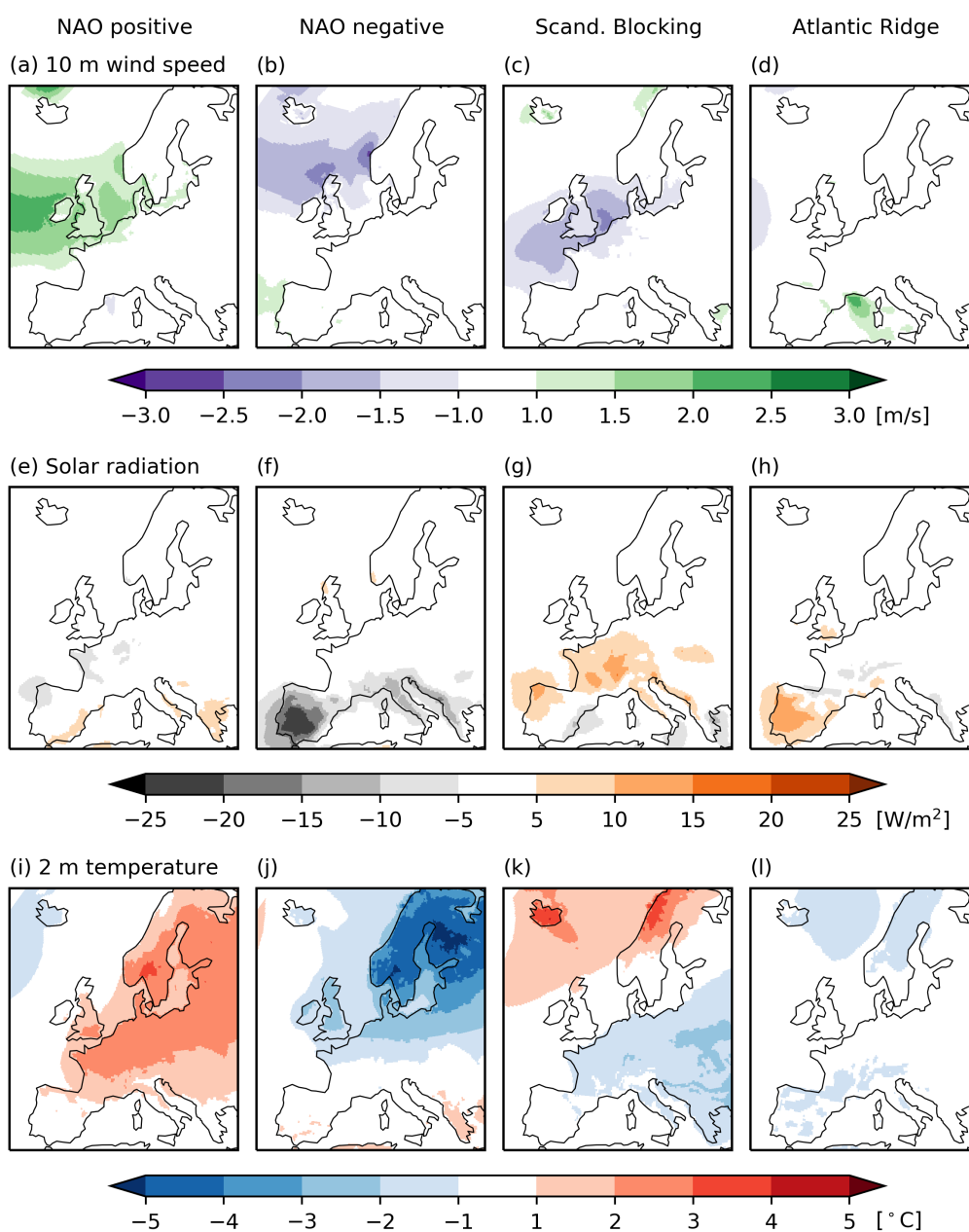


**Figure 2.** Mean meteorological surface impacts of the four weather regimes. Colours show anomalies of (a-d) 10 m wind speed [m/s], (e-h) incoming solar radiation [W/m<sup>2</sup>], (i-l) 2 m air temperature [°C]. Each weather regime in a column, labelled at the top, left to right: NAO positive, NAO negative, Scandinavian Blocking, Atlantic Ridge. Figure based on ERA5 data (DJF, 1979-2018).

227 (Figure 2d,l), incoming solar radiation is higher than normal over the Iberian Peninsula  
 228 (Figure 2h). Wind power potential is slightly higher than normal over the Mediterranean  
 229 Sea and North Sea (Figure 3d), solar power potential is higher than normal over the Iberian  
 230 Peninsula (Figure 3h).

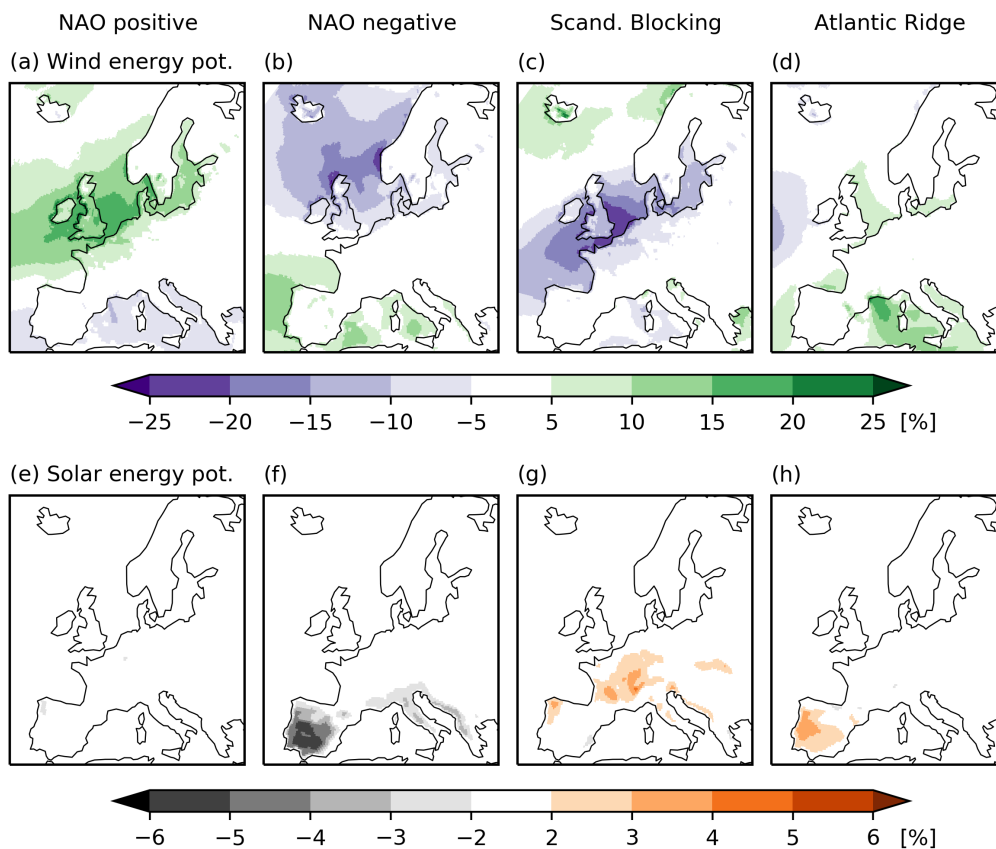


**Figure 3.** As Figure 2 but here for mean power production impacts of the four weather regimes. Colours show anomalies of (a-d) wind power potential [%], (e-h) solar power potential [%]. Each weather regime in a column, labelled at the top, left to right: NAO positive, NAO negative, Scandinavian Blocking, Atlantic Ridge. Figure based on ERA5 data (DJF, 1979-2018).

### 231 3.2. Energy related variability within weather regimes

232 For the investigation of variability within a weather regime, we reduce the spatial wind and  
 233 solar power potential data (as in Figure 3) to European totals, which results in time series for  
 234 wind and solar power production, energy demand and energy shortfall (see Section 2.3). On  
 235 average, total wind and solar power production is above normal in the NAO positive and the  
 236 Atlantic ridge regimes, and lower than normal in the NAO negative and Scandinavian Blocking  
 237 regimes (Figure 4a). Energy demand is below normal in NAO positive, but above normal in  
 238 the blocked regimes (Figure 4b). These results follow logically from the typical spatial patterns  
 239 of meteorological variables and power potentials discussed in the previous section.

240 Absolute variability is larger for wind and solar power production than for energy demand,  
 241 with standard deviations of 1.5 and 0.3 TWh day<sup>-1</sup> respectively. Consequently energy shortfall  
 242 more closely resembles the wind and solar energy production response than the energy demand  
 243 response, in agreement with Bloomfield et al. (2016). However, lower than normal production  
 244 coincides with higher than normal demand for days in NAO negative and Scandinavian  
 245 Blocking. Energy shortfall in those regimes is therefore higher than normal (Figure 4c), and  
 246 also higher than what would be estimated from wind and solar power production alone. NAO

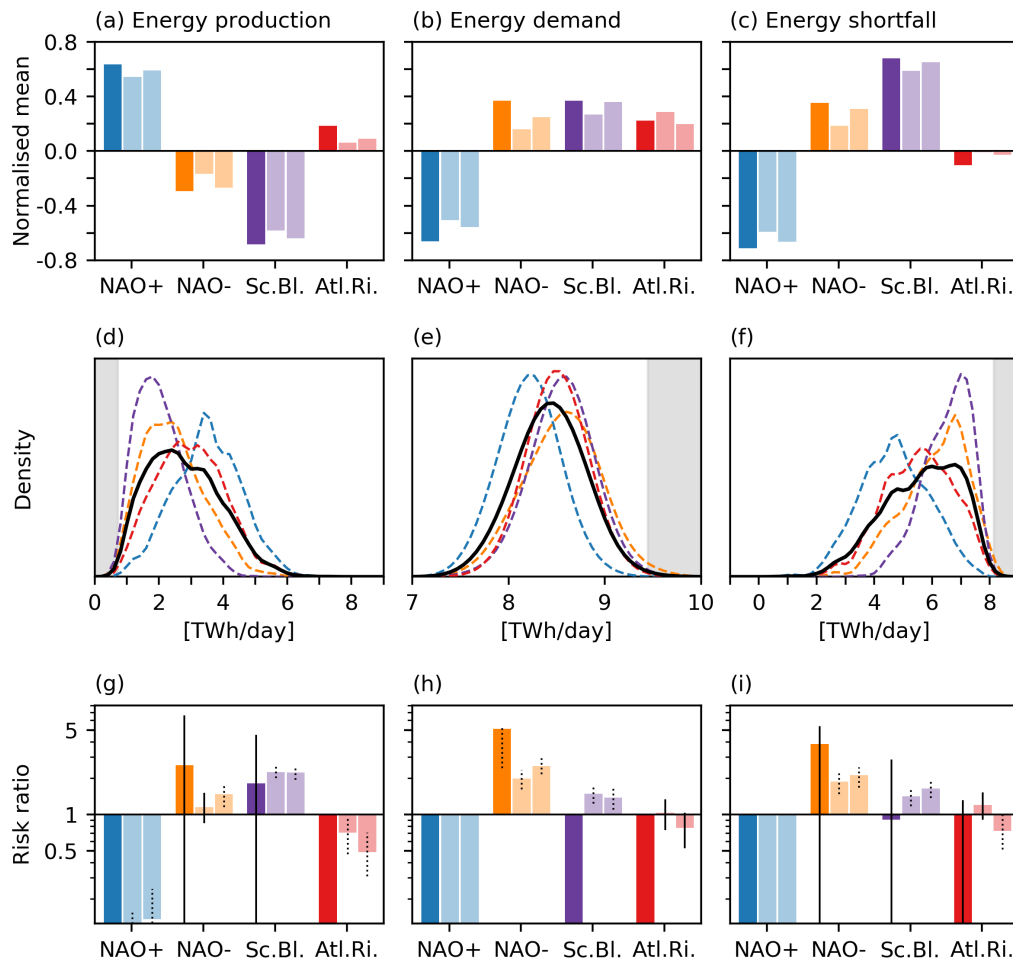


**Figure 4.** (a-c) Bar graphs showing the normalised mean of energy production/demand/shortfall for each weather regime relative to all winter days (normalised mean = 0, normalised standard deviation = 1) [no units]. (d-f) Distributions of European total energy production/demand/shortfall for all winter days (black solid line) and split by weather regime (coloured dashed lines, colours as in other panels) [TWh/day]. Grey shading denotes the threshold for the 1-in-10 year extreme event. (g-i) Risk ratio of 1-in-10 year extreme event occurrence conditional on the weather regime for energy production/demand/shortfall [no units]. Black vertical lines show the 95 % confidence interval based on bootstrap resampling ( $N=10,000$ ), a solid line when the change in risk is not statistically significant, a dotted line when the change is statistically significant. Subfigures (d-f) based on ERA5 data (DJF, 1979-2018), other subfigures (a-c, g-i) show ERA5 data in bold colours and large ensemble simulated data in lighter colours (DJF, 2000 years).

247 positive days typically combine above normal production with below normal demand, leading  
 248 to lower than normal energy shortfall. In the Atlantic Ridge regime both production and  
 249 demand are higher than normal, the resulting energy shortfall is close to being normal.

250 These average changes of the energy variables in each weather regime hide the variability  
 251 of these variables within a regime. Figures 4d-f (and SI Figure S4 for GCM data) show the  
 252 distribution of each energy variable for all winter days and split by regime. The distribution of

1  
2  
3  
4  
5  
6  
7  
8  
9  
10  
11  
12  
13  
14  
15  
16  
17  
18  
19  
20  
21  
22  
23  
24  
25  
26  
27  
28  
29  
30  
31  
32  
33  
34  
35  
36  
37  
38  
39  
40  
41  
42  
43  
44  
45  
46  
47  
48  
49  
50  
51  
52  
53  
54  
55  
56  
57  
58  
59  
60

wind and solar power production is positively skewed, indicating a long tail for high production values (Brayshaw et al., 2011; Zubiate et al., 2017). This distribution changes for each weather regime: in the Scandinavian Blocking regime the distribution shifts to lower values with increased skewness; during NAO positive the distribution shifts to higher values and is no longer skewed. The distribution of energy demand is normal, with each weather regime leading to a shift in the mean as discussed above. Energy shortfall is negatively skewed in the full distribution. Also here the largest changes in the distribution are for NAO positive (lower mean shortfall, no skewness) and Scandinavian Blocking (higher mean shortfall, increased skewness).

*3.2.1. Extreme energy events* Next we investigate the change in risk of extreme events for each weather regime. For this analysis we rely on the GCM large ensemble experiments, as noted in Section 2.1. Increased risk of extreme low wind and solar power production events is found for the Scandinavian Blocking regime and for NAO negative ( $RR = 2.2$  and  $1.3$  respectively, Figure 4g). Decreased risk is found for the NAO positive and Atlantic Ridge regimes ( $RR = 0.1$  and  $0.6$  respectively), though each GCM has some of the extreme events occurring in these regimes. Increased risk of extreme high energy demand is found for NAO negative, and Scandinavian Blocking ( $RR = 2.3$  and  $1.4$  respectively, Figure 4h). During Atlantic Ridge days there is a slight decrease of risk ( $RR = 0.9$ ). None of the sampled extreme high demand events occurred in the NAO positive regime, this does not imply that extreme high demand events are impossible in this regime, just very unlikely and not sampled here.

The risk of an extreme high energy shortfall event doubles during NAO negative days, and increases by 50 % in Scandinavian Blocking days ( $RR = 2.0$  and  $1.5$  respectively, Figure 4i). In the Atlantic Ridge regime the GCMs disagree on the sign of the small change of risk, on average there is no change in risk. In NAO positive the chance of extreme high energy shortfall is near zero, though in the GCM experiments three events occurred in this regime in 4000 simulated years.

The limited length of the ERA-Interim record hinders the ability to adequately sample extreme event occurrence and estimate changes in risk. For extreme low wind and solar energy production, the four sampled events are evenly distributed over the Scandinavian Blocking and NAO negative regimes (Figure 4g), this is in agreement with the increases in risk computed from the GCM data. This may lead to the false conclusion that such events do not occur on NAO positive or Atlantic Ridge days. The GCM experiments, by means of improved sampling, show that extreme low wind and solar energy production can occur in all regimes. Similar effects of limited sampling on the risk estimates are found for extreme high energy demand events and extreme high energy shortfall events (Figures 4h,i).

### *3.3. Meteorology of extreme high energy shortfall events*

We next investigate the meteorological conditions that cause the extreme high energy shortfall events (Figure 4i) in more detail, and compare these to the typical patterns associated with the weather regimes (Section 3.1). The 500 hPa circulation for a selection of simulated extreme shortfall events is shown in Figure 5. The resemblance between the event circulation and the regime centroid varies from event to event. In general, the large-scale pattern somewhat matches that of the regime centroid, higher pattern correlations are found for NAO negative events than for those classified in the other regimes. However, smaller-scale synoptic features cannot be disregarded.

To test if the circulation during extreme events systematically resembles the regime

centroids more/less than the circulation during normal days in the regime, we compare distributions of pattern correlations and anomaly magnitudes between daily circulation patterns and the regime centroids (SI Figures S5, S6). Taking into account all winter days, the pattern correlations vary between  $-0.17$  and  $0.95$  with an average value of  $0.48$ . A similar calculation based only on extreme high energy shortfall events results in a comparable distribution (mean  $0.53$ , range  $-0.02$  to  $0.88$ ). Also for anomaly magnitudes, compared by means of a projection onto the regime centroid, the distribution for extreme events is close to that of all winter days. Thus, within a regime, the days of extreme high energy shortfall are not distinct in terms of atmospheric circulation. Extreme shortfall events are not caused by extreme versions of the atmospheric circulation associated with the four weather regimes.

Despite different circulation patterns at 500 hPa, the events in Figure 5 all lead to extreme high energy shortfall. This is because the surface impacts of the events are remarkably similar (Figure 6). Each of the events shown is characterised by lower than normal winds over large parts of the continent and shallow seas due to low surface pressure gradients. In most events temperatures over the continent are lower than normal. Though the exact pattern and the strength of the anomalies of wind and temperature varies between events, it is obvious that all meteorological states lead to lower than normal wind power production and higher than normal energy demand, when combined resulting in extreme high energy shortfall.

There are no systematic differences between weather regimes (columns in Figure 6) if we consider surface meteorological conditions of extreme energy shortfall events. This is confirmed by an analysis of the pattern correlation of surface anomaly patterns of surface pressure, 10 m wind speed and 2 m temperature of the extreme high energy shortfall events over Europe (Figures 7b-d). These events are more similar to each other (composite mean pattern shown in Van der Wiel et al., 2019a, their Figure 9) than they are to their associated regime mean pattern (as in Figure 2). For 500 hPa circulation over the North-Atlantic European region, the meteorological parameter which formed the basis of the weather regime classification, the similarity between the event and regime centroid, and the event and the extreme event composite mean is comparable (Figure 7a).

#### 4. Summary

North Atlantic-European weather regimes have significant influence on meteorological surface conditions relevant for the energy sector. On average, wind and solar power production is above normal in the NAO positive and Atlantic Ridge regimes, and below normal in the Scandinavian Blocking and NAO negative regimes. Energy demand is higher than normal in the Scandinavian Blocking, NAO negative and Atlantic Ridge regimes. The combination of low production and high demand leads to higher than normal energy shortfall or residual load in the Scandinavian Blocking and NAO negative regimes. These results are in agreement with previous studies which looked at the average impacts of the NAO, the East Atlantic and the Scandinavian patterns, and weather regimes on wind power generation (e.g. Brayshaw et al., 2011; Ely et al., 2013; Grams et al., 2017; Zubiate et al., 2017) and energy demand (Thornton et al., 2019) separately. Similar results are obtained when repeating the analysis using ERA-Interim data (Dee et al., 2011).

However, these average effects hide large variability of meteorological conditions and energy impacts within each weather regime. For each weather regime, the changes to the full distribution of the three energy variables considered were analysed and used to quantify the resulting change in the risk of extreme events. For days classified as Scandinavian Blocking and NAO negative, the risk of extreme low wind and solar power production and extreme high

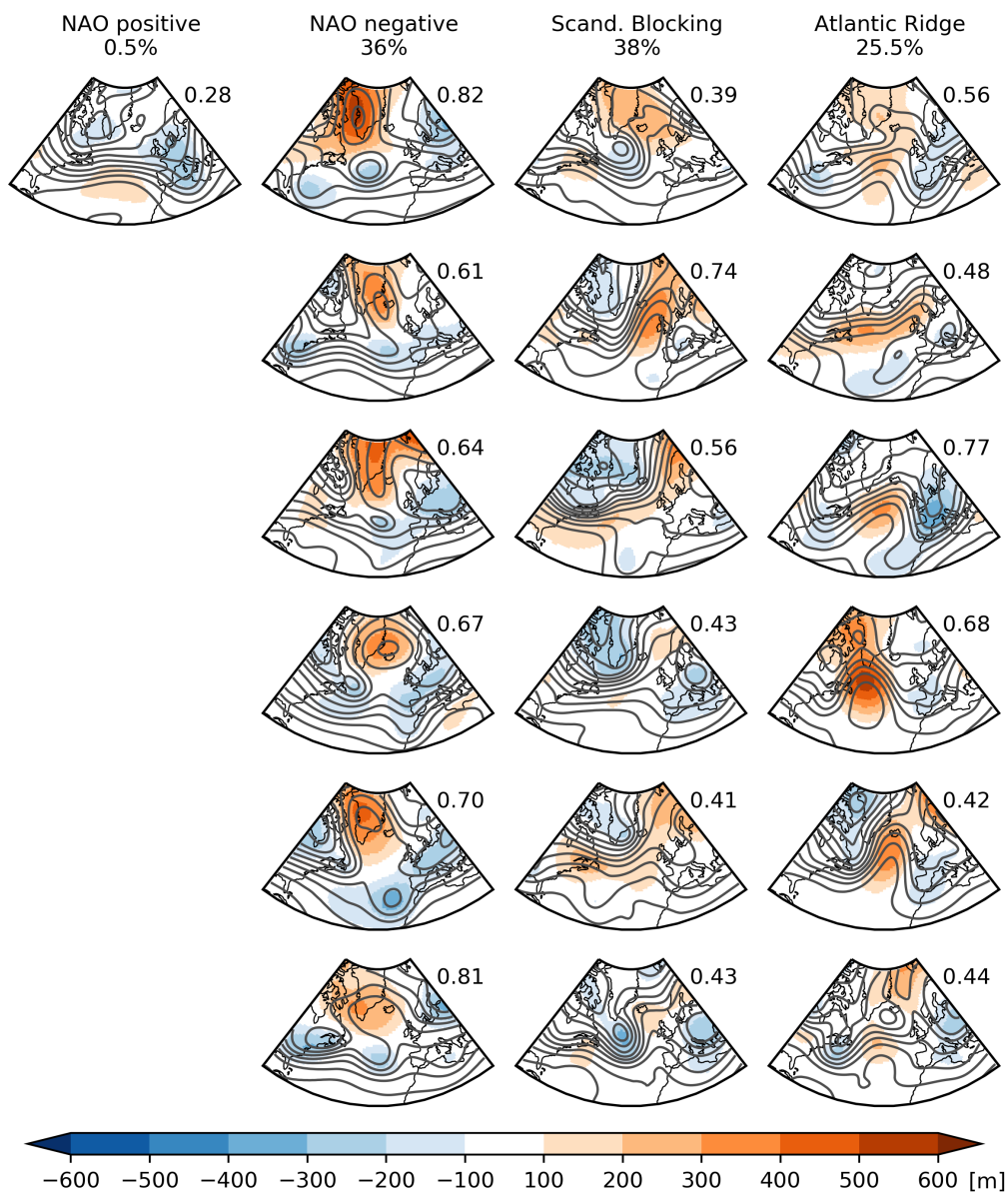


**Figure 5.** Atmospheric circulation pattern for the six most extreme high energy shortfall events in each weather regime (one event for NAO positive regime due to lower sampling). Colours show the 500 hPa geopotential height anomaly [m] (note different scale from Figure 1), contour lines show the 500 hPa height [m, interval 100 m] indicative of direction of flow. Each weather regime in a column, labelled at the top, left to right: NAO positive, NAO negative, Scandinavian Blocking, Atlantic Ridge. Percentage values at the top indicate the percentage of extreme events that fall in the regime, values to the right of each map show the pattern correlation coefficient between the pattern shown and the regime centroid (SI Figure S1). Figure based on the EC-Earth large ensemble experiment.

344 energy demand both increases, resulting in an increase of risk of extreme high energy shortfall  
 345 (by a factor of 2.0 and 1.5 respectively). Despite this preference for the blocked regimes (as  
 346 was characterized in Bloomfield et al. (2018) and Van der Wiel et al. (2019a)), extreme high

1  
2  
3  
4  
5  
6  
7  
8  
9  
10  
11  
12  
13  
14  
15  
16  
17  
18  
19  
20  
21  
22  
23  
24  
25  
26  
27  
28  
29  
30  
31  
32  
33  
34  
35  
36  
37  
38  
39  
40  
41  
42  
43  
44  
45  
46  
47  
48  
49  
50  
51  
52  
53  
54  
55  
56  
57  
58  
59  
60



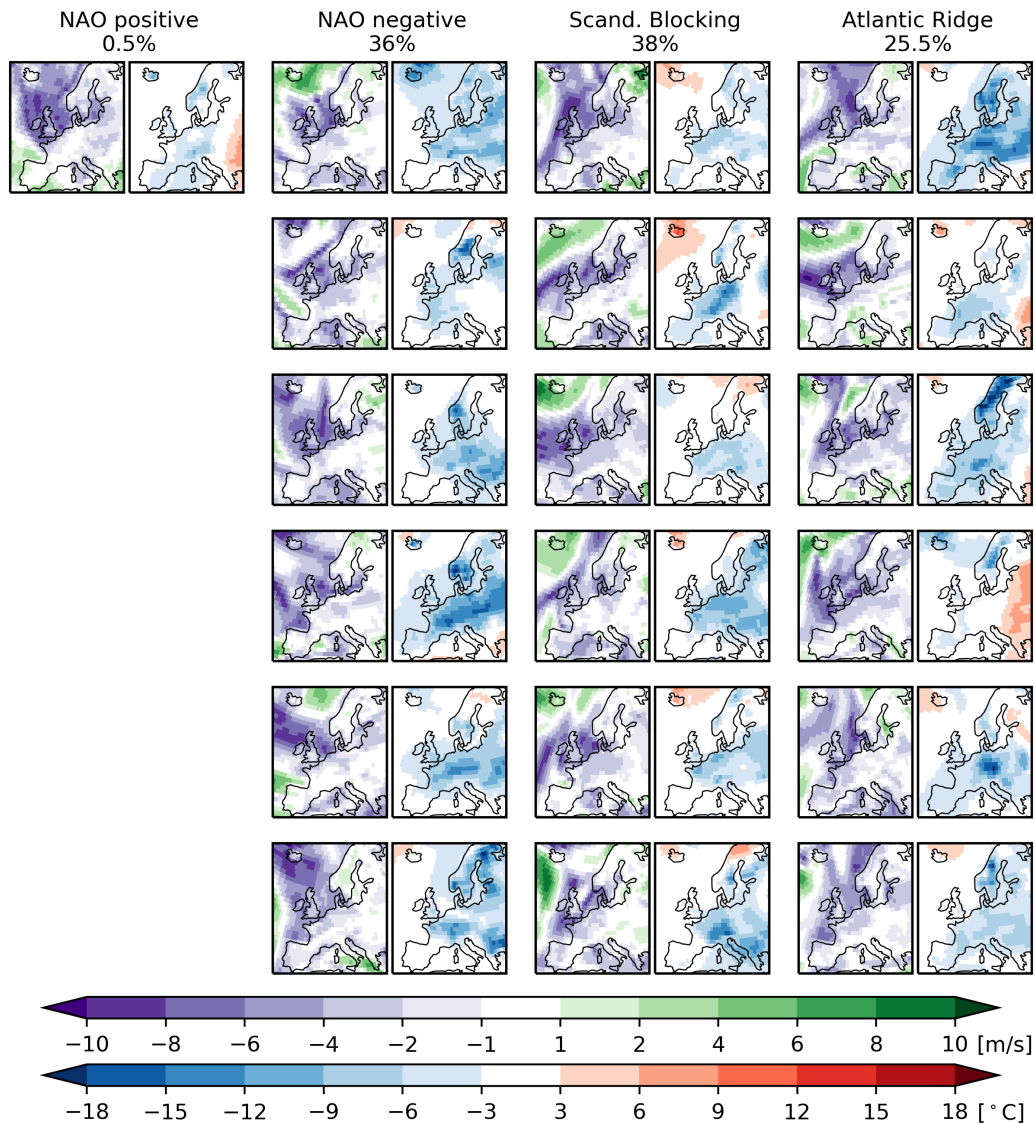


**Figure 6.** Meteorological surface conditions for the events shown in Figure 5. Purple/green colours show 10 m wind speed anomalies [m/s], blue/red colours show 2 m air temperature anomalies [°C] (note different scale from Figure 2). Figure based on the EC-Earth large ensemble experiment.

energy shortfall events occur in all four regimes. Finally, it is shown that the meteorological surface conditions leading to extreme shortfall events are more similar to each other than they are to their respective regime typical pattern. Extreme high energy shortfall events are caused by rare circulation types and smaller-scale synoptic features, rather than by extreme magnitudes of common circulation types (i.e. the weather regimes).

## 5. Conclusions

The aim of this study was to investigate whether weather regimes, a frequently used metric to simplify meteorological variability, capture the influence of meteorological variability on the European energy sector. Our analysis shows that some of the day-to-day variability of

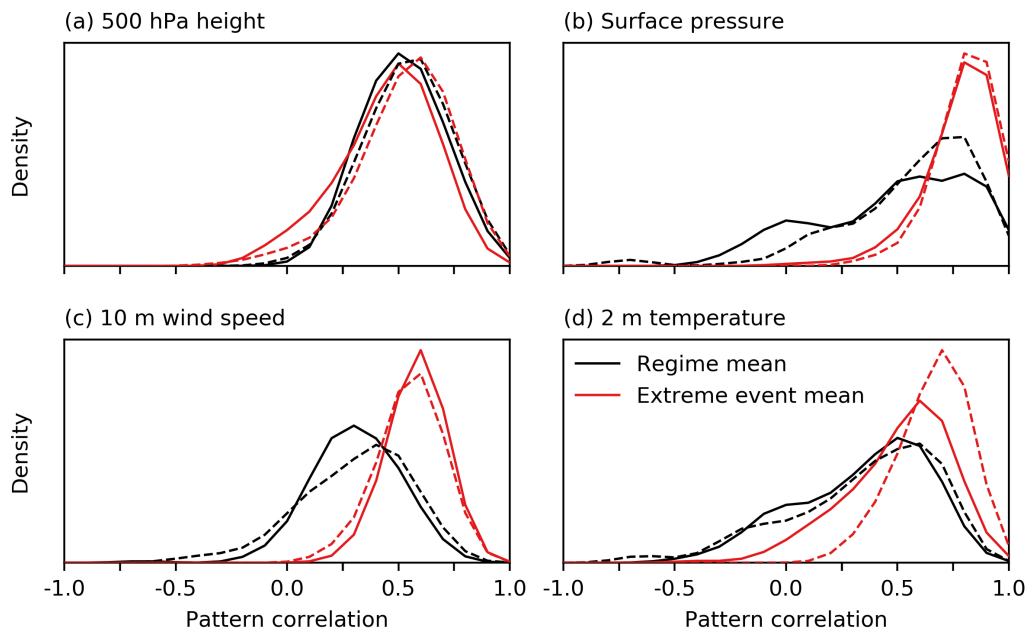


**Figure 7.** Distributions of pattern correlations for extreme high energy shortfall events for anomalies of (a) 500 hPa geopotential height, (b) surface pressure, (c) 10 m wind speed, (d) 2 m air temperature. Black lines show the distribution of correlation coefficients for the 200 events compared to their associated regime mean (as in Figures 1 and 2), red lines show the distribution of correlation coefficients for the 200 events compared to the extreme event composite mean. Correlations based on anomalies in (a) the North Atlantic-European region ( $90^{\circ}\text{W}$ - $30^{\circ}\text{E}$ ,  $20^{\circ}$ - $80^{\circ}\text{N}$ ), (b-d) a European region ( $15^{\circ}\text{W}$ - $35^{\circ}\text{E}$ ,  $25^{\circ}$ - $70^{\circ}\text{N}$ ). Figure based on the EC-Earth (solid lines) and HadGEM2-ES (dashed lines) large ensemble experiments.

energy variables can be explained by weather regimes, and hence they can be informative for the energy sector. For example, the probability of a given regime can be computed from meteorological forecasts at seasonal and sub-seasonal time scales, from which expected energy anomalies or changes in risk can be quantified. This extends NAO-based seasonal predictability for the energy sector (Clark et al., 2017; Thornton et al., 2019).

However, the analysis also shows there is substantial variability of energy variables within the weather regimes. Extreme energy events are the result of rare circulation types or smaller-scale features, not captured by these large-scale weather regimes. There is thus a limit to the precision of weather-regime based energy forecasts. Therefore we would advise to use the exact meteorology for forecasts of energy variables at shorter lead times or for, for example, system adequacy analyses.

Further work to improve scientific understanding of the link between weather and energy systems is required. A logical step following this analysis would be to try impact-centred or bottom-up analyses, in which regimes are defined based on their impact on energy variables rather than on the fraction of circulation variance explained (meteorology-centred or top-down). We hypothesise that such impact-based circulation regimes would exhibit less variability within regimes and would provide a better categorisation of extreme events. If such patterns can be shown to be predictable using existing meteorological forecasting systems, this would likely improve the value for the energy sector compared to forecasting based on



## REFERENCES

15

weather regimes as outlined above. From a meteorological perspective, further improvements may be possible when using smaller-scale synoptic-based European weather regimes (e.g. the 29 Großwetterlagen, James, 2007) or through unsupervised machine learning (e.g. as was done for Japan, Ohba et al., 2016). Finally, building on the present analysis, future work may investigate how the persistence of these four regimes influences the duration of high energy shortfall events. Longer lasting events put greater stress on energy systems (Van der Wiel et al., 2019a).

382 **Acknowledgments**

This work is part of the HiWAVES3 project, funding was supplied by the Netherlands Organisation of Scientific Research (NWO) under grant number ALWCL.2016.2. HCB is funded by H2020-EU.3.5.1 grant 776787. RWL is funded by NERC grant NE/P00678/1. LPS is funded by NWO under grant number 647.003.005. Results were generated using the Copernicus Climate Change Service Information 2019, neither the European Commission nor ECMWF are responsible for the statements, findings, conclusions and recommendations. The authors thank two anonymous reviewers for their comments.

390 **Data availability**

The ERA5 data used in this study can be downloaded from the Copernicus Climate Change Service Climate Data Store <https://cds.climate.copernicus.eu/cdsapp#!/home>. Climate model data is available on reasonable request from the corresponding author.

394 **References**

- Armaroli, N., and V. Balzani, 2011: Towards an electricity-powered world. *Energy & Environmental Science*, **4** (9), 3193–3222, doi:10.1039/C1EE01249E.
- Bessec, M., and J. Fouquau, 2008: The non-linear link between electricity consumption and temperature in Europe: a threshold panel approach. *Energy Economics*, **30** (5), 2705–2721, doi:10.1016/j.eneco.2008.02.003.
- Blackport, R., and J. A. Screen, 2019: Influence of Arctic sea-ice loss in autumn compared to that in winter on the atmospheric circulation. *Geophysical Research Letters*, **46**, 2213–2221, doi:10.1029/2018GL081469.
- Bloomfield, H. C., D. J. Brayshaw, L. C. Shaffrey, P. J. Coker, and H. E. Thornton, 2016: Quantifying the increasing sensitivity of power systems to climate variability. *Environmental Research Letters*, **11** (12), 124025, doi:10.1088/1748-9326/11/12/124025.
- Bloomfield, H. C., D. J. Brayshaw, L. C. Shaffrey, P. J. Coker, and H. E. Thornton, 2018: The changing sensitivity of power systems to meteorological drivers: a case study of Great Britain. *Environmental Research Letters*, **13** (5), 054028, doi:10.1088/1748-9326/aabff9.
- Brayshaw, D. J., A. Troccoli, R. Fordham, and J. Methven, 2011: The impact of large scale atmospheric circulation patterns on wind power generation and its potential predictability: A case study over the uk. *Renewable Energy*, **36** (8), 2087–2096, doi:10.1016/j.renene.2011.01.025.
- Cassou, C., 2008: Intraseasonal interaction between the Madden–Julian oscillation and the North Atlantic Oscillation. *Nature*, **455** (7212), 523, doi:10.1038/nature07286.

## REFERENCES

16

- 415 Clark, R. T., P. E. Bett, H. E. Thornton, and A. A. Scaife, 2017: Skilful seasonal predictions  
416 for the European energy industry. *Environmental Research Letters*, **12** (2), 024002, doi:  
417 10.1088/1748-9326/aa57ab.
- 418 Copernicus Climate Change Service, 2017: ERA5: Fifth generation of ECMWF atmospheric  
419 reanalyses of the global climate. Copernicus Climate Change Service Climate Data Store  
420 (CDS), accessed June 2019, <https://cds.climate.copernicus.eu/cdsapp#!/home>.
- 421 Craig, M. T., I. L. Carreño, M. Rossol, B.-M. Hodge, and C. Brancucci, 2019: Effects on  
422 power system operations of potential changes in wind and solar generation potential under  
423 climate change. *Environmental Research Letters*, **14** (3), 034014.
- 424 Curtis, J., M. Á. Lynch, and L. Zubiate, 2016: The impact of the North Atlantic Oscillation  
425 on electricity markets: A case study on Ireland. *Energy Economics*, **58**, 186–198, doi:  
426 10.1016/j.eneco.2016.07.003.
- 427 Davy, R. J., and A. Troccoli, 2012: Interannual variability of solar energy generation in  
428 Australia. *Solar Energy*, **86** (12), 3554–3560, doi:10.1016/j.solener.2011.12.004.
- 429 Dawson, A., 2016: eofs: A library for eof analysis of meteorological, oceanographic, and climate  
430 data. *Journal of Open Research Software*, **4** (1).
- 431 Dee, D. P., and Coauthors, 2011: The ERA-Interim reanalysis: configuration and performance  
432 of the data assimilation system. *Quarterly Journal of the Royal Meteorological Society*,  
433 **137** (656), 553–597, doi:10.1002/qj.828.
- 434 Donat, M. G., G. C. Leckebusch, J. G. Pinto, and U. Ulbrich, 2010: Examination of wind  
435 storms over Central Europe with respect to circulation weather types and NAO phases.  
436 *International Journal of Climatology*, **30** (9), 1289–1300, doi:10.1002/joc.1982.
- 437 Ely, C. R., D. J. Brayshaw, J. Methven, J. Cox, and O. Pearce, 2013: Implications of the  
438 North Atlantic Oscillation for a UK–Norway renewable power system. *Energy Policy*, **62**,  
439 1420–1427, doi:10.1016/j.enpol.2013.06.037.
- 440 Ferranti, L., S. Corti, and M. Janousek, 2015: Flow-dependent verification of the ECMWF  
441 ensemble over the Euro-Atlantic sector. *Quarterly Journal of the Royal Meteorological  
442 Society*, **141** (688), 916–924.
- 443 Grams, C. M., R. Beerli, S. Pfenninger, I. Staffell, and H. Wernli, 2017: Balancing Europes  
444 wind-power output through spatial deployment informed by weather regimes. *Nature climate  
445 change*, **7** (8), 557, doi:10.1038/nclimate3338.
- 446 Haupt, S. E., J. Copeland, W. Y. Cheng, Y. Zhang, C. Ammann, and P. Sullivan, 2016: A  
447 method to assess the wind and solar resource and to quantify interannual variability over the  
448 United States under current and projected future climate. *Journal of Applied Meteorology  
449 and Climatology*, **55** (2), 345–363.
- 450 Hazeleger, W., and Coauthors, 2012: EC-Earth V2.2: description and validation of a new  
451 seamless Earth system prediction model. *Climate dynamics*, **39** (11), 2611–2629, doi:  
452 10.1007/s00382-011-1228-5.
- 453 Huber, M., D. Dimkova, and T. Hamacher, 2014: Integration of wind and solar power in  
454 Europe: Assessment of flexibility requirements. *Energy*, **69**, 236–246, doi:10.1016/j.energy.  
455 2014.02.109.
- 456 Hueging, H., R. Haas, K. Born, D. Jacob, and J. G. Pinto, 2013: Regional changes in wind  
457 energy potential over Europe using regional climate model ensemble projections. *Journal of  
458 Applied Meteorology and Climatology*, **52** (4), 903–917, doi:10.1175/JAMC-D-12-086.1.

## REFERENCES

17

- Hurrell, J. W., Y. Kushnir, G. Ottersen, and M. Visbeck, 2003: An overview of the North Atlantic oscillation. *The North Atlantic Oscillation: climatic significance and environmental impact*, **134**, 1–35.
- James, P., 2007: An objective classification method for Hess and Brezowsky Großwetterlagen over Europe. *Theoretical and Applied Climatology*, **88** (1-2), 17–42, doi:10.1007/s00704-006-0239-3.
- Jerez, S., F. Thais, I. Tobin, M. Wild, A. Colette, P. Yiou, and R. Vautard, 2015a: The CLIMIX model: a tool to create and evaluate spatially-resolved scenarios of photovoltaic and wind power development. *Renewable and Sustainable Energy Reviews*, **42**, 1–15, doi:10.1016/j.rser.2014.09.041.
- Jerez, S., R. M. Trigo, S. M. Vicente-Serrano, D. Pozo-Vázquez, R. Lorente-Plazas, J. Lorenzo-Lacruz, F. Santos-Alamillos, and J. Montávez, 2013: The impact of the North Atlantic Oscillation on renewable energy resources in southwestern Europe. *Journal of applied meteorology and climatology*, **52** (10), 2204–2225, doi:10.1175/JAMC-D-12-0257.1.
- Jerez, S., and Coauthors, 2015b: The impact of climate change on photovoltaic power generation in Europe. *Nature communications*, **6**, 10 014, doi:10.1038/ncomms10014.
- Kavak Akpınar, E., and S. Akpınar, 2005: An assessment on seasonal analysis of wind energy characteristics and wind turbine characteristics. *Energy conversion and management*, **46** (11-12), 1848–1867, doi:10.1016/j.enconman.2004.08.012.
- Klink, K., 2002: Trends and interannual variability of wind speed distributions in Minnesota. *Journal of Climate*, **15** (22), 3311–3317.
- Kumler, A., I. L. Carreno, M. Craig, B.-M. Hodge, W. Cole, and C. Brancucci, 2018: Inter-annual variability of wind and solar electricity generation and capacity values in texas. *Environmental Research Letters*.
- Lavaysse, C., J. Vogt, A. Toreti, M. L. Carrera, and F. Pappenberger, 2018: On the use of weather regimes to forecast meteorological drought over Europe. *Natural Hazards and Earth System Sciences*, **18** (12), 3297–3309, doi:10.5194/nhess-18-3297-2018.
- Martin, G. M., and Coauthors, 2011: The HadGEM2 family of met office unified model climate configurations. *Geoscientific Model Development*, **4** (3), 723–757, doi:10.5194/gmd-4-723-2011.
- Matsueda, M., and T. Palmer, 2018: Estimates of flow-dependent predictability of wintertime Euro-Atlantic weather regimes in medium-range forecasts. *Quarterly Journal of the Royal Meteorological Society*, **144** (713), 1012–1027, doi:10.1002/qj.3265.
- Matthews, H. D., N. P. Gillett, P. A. Stott, and K. Zickfeld, 2009: The proportionality of global warming to cumulative carbon emissions. *Nature*, **459** (7248), 829, doi:10.1038/nature08047.
- Meinshausen, M., N. Meinshausen, W. Hare, S. C. Raper, K. Frieler, R. Knutti, D. J. Frame, and M. R. Allen, 2009: Greenhouse-gas emission targets for limiting global warming to 2 °C. *Nature*, **458** (7242), 1158, doi:10.1038/nature08017.
- Michelangeli, P.-A., R. Vautard, and B. Legras, 1995: Weather regimes: Recurrence and quasi stationarity. *Journal of the atmospheric sciences*, **52** (8), 1237–1256, doi:10.1175/1520-0469(1995)052<1237:WRRAS>2.0.CO;2.
- Neal, R., D. Fereday, R. Crocker, and R. E. Comer, 2016: A flexible approach to defining weather patterns and their application in weather forecasting over europe. *Meteorological Applications*, **23** (3), 389–400, doi:0.1002/met.1563.

## REFERENCES

18

- Ohba, M., S. Kadokura, and D. Nohara, 2016: Impacts of synoptic circulation patterns on wind power ramp events in East Japan. *Renewable energy*, **96**, 591–602, doi:10.1016/j.renene.2016.05.032.
- Olauson, J., 2018: ERA5: The new champion of wind power modelling? *Renewable energy*, **126**, 322–331.
- Pedregosa, F., and Coauthors, 2011: Scikit-learn: Machine learning in Python. *Journal of Machine Learning Research*, **12**, 2825–2830.
- Pinson, P., and Coauthors, 2013: Wind energy: Forecasting challenges for its operational management. *Statistical Science*, **28** (4), 564–585.
- Plaut, G., and E. Simonnet, 2001: Large-scale circulation classification, weather regimes, and local climate over France, the Alps and Western Europe. *Climate Research*, **17** (3), 303–324, doi:10.3354/cr017303.
- Pozo-Vázquez, D., J. Tovar-Pescador, S. Gámiz-Fortis, M. Esteban-Parra, and Y. Castro-Díez, 2004: NAO and solar radiation variability in the European North Atlantic region. *Geophysical Research Letters*, **31** (5), doi:10.1029/2003GL018502.
- Pryor, S. C., and R. J. Barthelmie, 2010: Climate change impacts on wind energy: a review. *Renewable and sustainable energy reviews*, **14** (1), 430–437, doi:10.1016/j.rser.2009.07.028.
- Pryor, S. C., R. J. Barthelmie, and J. T. Schoof, 2006: Inter-annual variability of wind indices across Europe. *Wind Energy*, **9** (1-2), 27–38, doi:10.1002/we.178.
- Ramon, J., L. Lledó, V. Torralba, A. Soret, and F. Doblas-Reyes, 2019: What global reanalysis best represents near surface winds? *Quarterly Journal of the Royal Meteorological Society*, doi:10.1002/qj.3616, in press.
- Ravestein, P., G. van der Schrier, R. Haarsma, R. Scheele, and M. van den Broek, 2018: Vulnerability of European intermittent renewable energy supply to climate change and climate variability. *Renewable and Sustainable Energy Reviews*, **97**, 497 – 508, doi:https://doi.org/10.1016/j.rser.2018.08.057.
- Reinhold, B., 1987: Weather regimes: the challenge in extended-range forecasting. *Science*, **235** (4787), 437–441, doi:10.1126/science.235.4787.437.
- Reyers, M., J. Moemken, and J. G. Pinto, 2016: Future changes of wind energy potentials over Europe in a large CMIP5 multi-model ensemble. *International Journal of Climatology*, **36** (2), 783–796, doi:10.1002/joc.4382.
- Sanchez-Gomez, E., S. Somot, and M. Déqué, 2009: Ability of an ensemble of regional climate models to reproduce weather regimes over Europe-Atlantic during the period 1961–2000. *Climate Dynamics*, **33** (5), 723–736, doi:10.1007/s00382-008-0502-7.
- Santos, J., J. Corte-Real, and S. Leite, 2005: Weather regimes and their connection to the winter rainfall in Portugal. *International Journal of Climatology*, **25** (1), 33–50.
- Sinden, G., 2007: Characteristics of the UK wind resource: Long-term patterns and relationship to electricity demand. *Energy Policy*, **35** (1), 112–127, doi:10.1016/j.enpol.2005.10.003.
- Suri, M., T. A. Huld, E. D. Dunlop, and H. A. Ossenbrink, 2007: Potential of solar electricity generation in the European Union member states and candidate countries. *Solar energy*, **81** (10), 1295–1305, doi:10.1016/j.solener.2006.12.007.
- Tamizhmani, G., L. Ji, Y. Tang, L. Petacci, and C. Osterwald, 2003: Photovoltaic module thermal/wind performance: long-term monitoring and model development for energy rating. *NCPV and solar program review meeting*, NREL, Vol. 2003.

## REFERENCES

19

- 549 Thornton, H. E., A. Scaife, B. J. Hoskins, D. J. Brayshaw, D. Smith, N. Dunstone, N. Stringer,  
550 and P. E. Bett, 2019: Skilful seasonal prediction of winter gas demand. *Environmental*  
551 *Research Letters*, **14** (2), 024 009, doi:10.1088/1748-9326/aaf338.
- 552 Thornton, H. E., A. A. Scaife, B. J. Hoskins, and D. J. Brayshaw, 2017: The relationship  
553 between wind power, electricity demand and winter weather patterns in great britain.  
554 *Environmental Research Letters*, **12** (6), 064 017.
- 555 Trigo, R. M., and C. C. DaCamara, 2000: Circulation weather types and their influence on the  
556 precipitation regime in Portugal. *International Journal of Climatology*, **20** (13), 1559–1581,  
557 doi:10.1002/1097-0088(20001115)20:13<1559::AID-JOC555>3.0.CO;2-5.
- 558 Urraca, R., T. Huld, A. Gracia-Amillo, F. J. Martinez-de Pison, F. Kaspar, and A. Sanz-  
559 Garcia, 2018: Evaluation of global horizontal irradiance estimates from ERA5 and COSMO-  
560 REA6 reanalyses using ground and satellite-based data. *Solar Energy*, **164**, 339–354.
- 561 Van der Wiel, K., L. P. Stoop, B. R. H. Van Zuijlen, R. Blackport, M. A. Van den Broek, and  
562 F. M. Selten, 2019a: Meteorological conditions leading to extreme low variable renewable  
563 energy production and extreme high energy shortfall. *Renewable and Sustainable Energy*  
564 *Reviews*, **111**, 261–275, doi:10.1016/j.rser.2019.04.065.
- 565 Van der Wiel, K., N. Wanders, F. M. Selten, and M. F. P. Bierkens, 2019b: Added value of  
566 large ensemble simulations for assessing extreme river discharge in a 2 °C warmer world.  
567 *Geophysical Research Letters*, **46**, 2093–2102, doi:10.1029/2019GL081967.
- 568 Vautard, R., 1990: Multiple weather regimes over the North Atlantic: analysis of precursors  
569 and successors. *Monthly weather review*, **118** (10), 2056–2081, doi:10.1175/1520-0493(1990)  
570 118(2056:MWROTN)2.0.CO;2.
- 571 Yiou, P., K. Goubanova, Z. Li, and M. Nogaj, 2008: Weather regime dependence of  
572 extreme value statistics for summer temperature and precipitation. *Nonlinear Processes*  
573 *in Geophysics*, **15** (3), 365–378, doi:10.5194/npg-15-365-2008.
- 574 Yiou, P., and M. Nogaj, 2004: Extreme climatic events and weather regimes over the  
575 North Atlantic: When and where? *Geophysical Research Letters*, **31** (7), doi:10.1029/  
576 2003GL019119.
- 577 Zeyringer, M., J. Price, B. Fais, P.-H. Li, and E. Sharp, 2018: Designing low-carbon power  
578 systems for Great Britain in 2050 that are robust to the spatiotemporal and inter-annual  
579 variability of weather. *Nature Energy*, **3** (5), 395, doi:10.1038/s41560-018-0128-x.
- 580 Zubiate, L., F. McDermott, C. Sweeney, and M. O'Malley, 2017: Spatial variability in winter  
581 NAO–wind speed relationships in western Europe linked to concomitant states of the East  
582 Atlantic and Scandinavian patterns. *Quarterly Journal of the Royal Meteorological Society*,  
583 **143** (702), 552–562, doi:10.1002/qj.2943.